INNOVARE JOURNAL OF MEDICAL SCIENCES

Vol 10, Issue 6, 2022

ISSN - 2321-4406

Research Article

COMPUTATIONAL ANALYSIS OF PHYTOCOMPOUNDS PRESENT IN *MURRAYA KOENIGII* TO TARGET *HAEMOPHILUS INFLUENZAE* DISEASE

AARSHA GANESH*

Department of Biotechnology, N.M.A.M Institute of Technology, Nitte, Karnataka, India. Email: aarshaganesh12@gmail.com

Received: 15 October 2022, Revised and Accepted: 25 October 2022

ABSTRACT

Objective: *Haemophilus influenzae* is a key contributor to meningitis, pneumonia, and sepsis-related illnesses and fatalities in children around the world during the pre-vaccine era (the early 1990s) and still continues to infect many individuals across the globe. This research examines various bioactive substances from plant sources for the prediction of the efficacy of the plant-based ligands to combat *H. influenzae.*

Methods: The present study implemented computational methods to assess the effectiveness of several phytochemicals toward the *H. influenzae* protein. The virtual screening tool PyRx was used to systematically perform molecular docking. To test the binding affinity with the *H. influenzae* protein 3ZH5, 10 phytocompounds were selected from *Murraya koenigii* based on the previous literature. Using ADMET filters, the pharmacological evaluation of the ligands was performed.

Results: The plant *M. koenigii*'s phytocompounds Mahanimbine, Murrayacinine, and Murrayazolinine were found to be the most effective antagonists for the protein 3ZH5, according to the docking data.

Conclusion: Due to their high affinity for the protein, all of these bioactive substances could be considered as deserving candidates for the suppression of *H. influenzae*.

Keywords: *Haemophilus influenzae*, 3ZH5 protein, *Murraya koenigii*, Phytocompounds.

 DOI: http://dx.doi.org/10.22159/ijms.2022v10i6.46621. Journal homepage: https://innovareacademics.in/journals/index.php/ijms

INTRODUCTION

Haemophilus influenzae, a coccobacillus that belongs to the *Pasteurellaceae* family, is a facultatively anaerobic, nonmotile, Gram-negative bacterium that requires the growth factors hemin (factor X) and NAD to flourish (factor V). Depending on whether a polysaccharide capsule is present or not, *H. influenzae* strains are split into two groups, that is, encapsulated and unencapsulated strains. Infants and kids suffer invasive infections from serotype B strains. Nontypeable strains usually infect children and adults' mucous membranes and colonize the upper respiratory tract. Numerous virulence factors, such as adhesins, nutrition absorption systems, and molecules that resist host influences, and others, mediate colonization and infection. The upper respiratory tract infections caused by *H. influenzae* are Otitis media in children, Sinusitis, and Conjunctivitis. The lower respiratory tract infections are Exacerbations in adults with chronic obstructive pulmonary disease, Pneumonia, and Infections in Cystic Fibrosis [1].

The multifunctional adhesin known as *H. influenzae* protein E (PE) (Fig. 1) interacts directly with host proteins such as plasminogen and the extracellular matrix proteins vitronectin and laminin as well as lung epithelial cells. PE is a 16-kDa surface lipoprotein. It induces an inflammatory response during infection, resulting in the secretion of interleukin 8 (IL-8) and increased expression of ICAM-1 (CD54) in both cell lines and primary epithelial cells. The structural discoveries shed light on the areas that engage with host proteins and suggest a potential method by which *H. influenzae* interacts with its host through PE [2].

Herbalists believe that medicinal plants have certain therapeutic qualities. In rural and tribal regions, they serve as the readily accessible source of healthcare. The medicinal plant used in this study is *Murraya koenigii* (Fig. 2) for which the common name is curry leaves. This plant is frequently used as a spice, herb, and condiment as well as a traditional treatment for a number of illnesses in India [3]. *M. koenigii* exhibits a wide range of traits, including antibacterial, antifungal, and antiprotozoal activity [4].

Over the past 20 years, a number of *H. influenzae* clinical manifestations have experienced significant alterations. In areas where the vaccines are extensively used, the development and use of *H. influenzae* type b (Hib) conjugate vaccines have virtually eliminated invasive Hib illness in children [1]. In this study, we will examine which *M. koenigii* phytocompounds have the highest binding affinities to the *H. influenzae* PE.

METHODS

In search of a lead that might inhibit *H. influenzae*, extensive virtual screening and molecular docking studies were done to identify the most promising therapeutic targets against the 3ZH5 protein.

Retrieval of protein

The surface lipoprotein *H. influenzae* PE with PDB ID 3ZH5 was downloaded from the RCSB PDB databank (https://www.rcsb.org/structure/3ZH5). The protein is downloaded in the.PDB format [5-8]. The resolution of the protein downloaded is 1.8Å and the method of retrieval of the protein is X-ray diffraction (Fig. 1).

Protein structure analysis and purification

Protein 3ZH5 was purified by adding polar hydrogen atoms and removing ligand groups and hetero atoms. The water molecule's free energy does not correspond to its crystallographic structure. Water molecules were completely removed before docking because they can alter docking scores. The prebound ligands are taken out of the crystal structures to speed up binding with the ligands selected for the investigation. While other chains were eliminated from the protein structures to make them simpler, Chain A was left intact for examination. To improve the quality of purified structures, polar hydrogen atoms are added.

The purified protein was uploaded to the Zlab Ramachandran server (https://zlab.umassmed.edu/bu/rama/) to construct the Ramachandran plot (Fig. 3). Further, the purified protein was uploaded to EMBOSS Pepwindow (https://www.ebi.ac.uk/Tools/seqstats/emboss_pepwindow/) and a hydropathy plot was obtained (Fig. 4). EMBOSS Pepstats (Table 1) (https://www.ebi.ac.uk/Tools/seqstats/emboss_pepstats/) and PDBsum (http://www.ebi.ac.uk/thornton-srv/databases/pdbsum/Generate.html) were employed to predict the secondary structures (Fig. 5) [9,10].

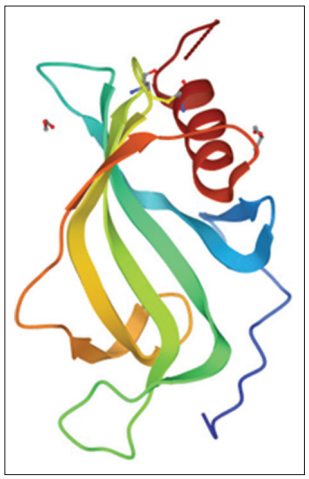

Fig. 1: Structure of *H.influenzae* protein E(3ZH5)

Fig. 2: *Murraya koenigii* leaves

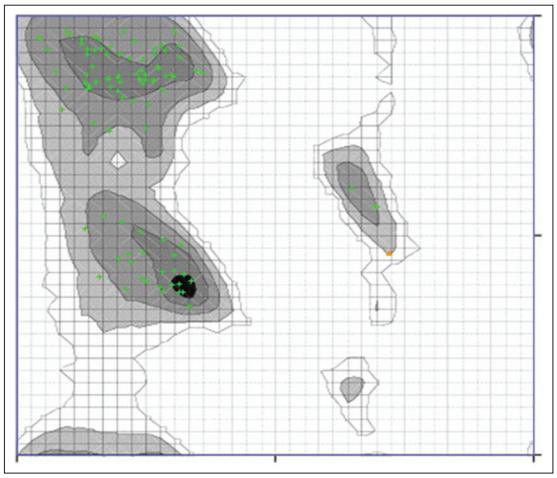

Fig. 3: Ramachandran plot of 3ZH5 protein using Zlab Ramachandran server

Retrieval of ligands

Based on the previous literature that examined the pharmacological characteristics of *M. koenigii* 10 ligands were chosen for the investigation. Potential ligands were sought using the IMPPAT (Indian Medicinal Plants, Phytochemistry and Therapeutics) database (https://cb.imsc.res.in/imppat/home). All of the ligands chosen for the current investigation had their canonical smiles recorded. The top three ligands were downloaded in.SDF format from PubChem (https://pubchem.ncbi.nlm.nih.gov/) [8,11,12].

Pharmacological studies

To assess the ligands' pharmacological characteristics, SwissADME (http://www.swissadme.ch/) analysis is tabulated (Table 2) [13]. The physicochemical qualities evaluated are Lipophilicity, Polarity, Insolubility, Size, Flexibility, and Instauration (Table 3). The BOILED-Egg was produced after analysis of the pharmacokinetic and medicinal chemistry properties (Fig. 6). The best ligands are then chosen using the LIPINSKI rule of 5 (Table 4) [14,15].

ChemAGG (https://admet.scbdd.com/ChemAGG/index/) is used to examine the ligand aggregation (Table 5) [16]. ProTox-II (https://tox-new.charite.de/protox_II/) is utilized to assess the toxicological characteristics (Table 6).

Molecular docking

From the RCSB PDB database, the protein 3ZH5 is downloaded in.PDB format. Based on their pharmacological significance and drug-like qualities, the top 3 ligands were chosen for additional examination. Using the OPENBABEL Chemical file format converter, the ligands were

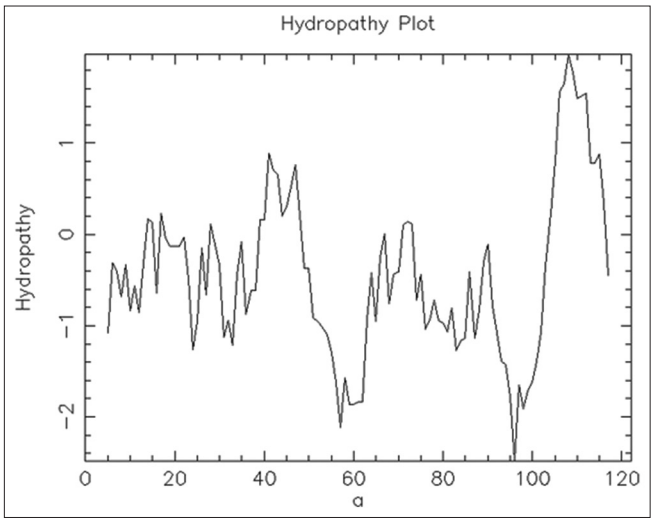

Fig. 4: Hydropathy plot of the protein 3ZH5

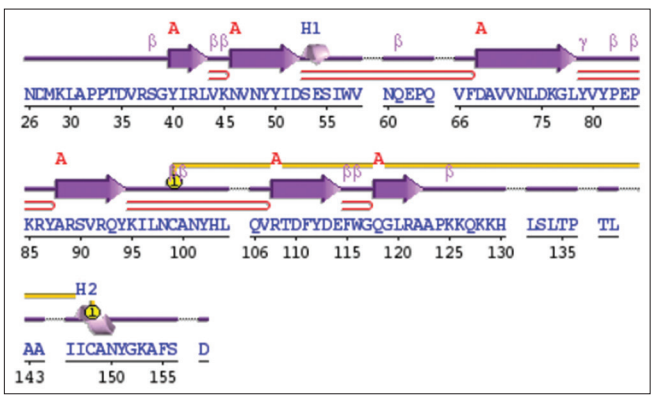

Fig. 5: Secondary structure of protein 3ZH5 using PDBsum

changed from.SDF format to.PDB format [17,18]. Active site dimensions were set as grid size of center X=37.4548Å, center Y=38.2739Å, and center Z=52.2141Å. Using the PyRx web server, the ligands were docked separately against 3ZH5 [19]. In PyRx the purified protein was loaded as a macromolecule and the phytocompounds of the plant were loaded as ligands. Energy minimization was performed and the ligands were docked. Once the docking results were obtained, suitable compounds with the most binding affinity, that is, Mahanimbine, Murrayazolinine, and Murrayacinine were chosen for further analysis based on their binding affinity with the target protein.

Visualization

The conformations with the best binding score were downloaded in.PDB format and visualized using Dassault Systems BIOVIA Discovery Studio Visualizer and the 2D, as well as 3D models, were obtained [20] (Fig. 7-9).

RESULTS

Protein structure analysis

Black, dark grey, grey, and light grey represent highly preferred conformations. White with black grid represents preferred conformations. White with grey grid represents questionable conformations. Highly preferred conformations are shown as green crosses, that is, 98.99%. Preferred observations are shown as brown triangles, that is, 1.010% and questionable observations are shown as red circles which are 0.00% in this study.

Table 1: Properties of protein obtained using Pepstats

Property	Residues	Number	Mole%
Tiny	(A+C + G+S + T)	114	29.381
Small	(A+B + C+D + G+N + P+S + T+V)	205	52.835
Aliphatic	(A+I + L+V+)	124	31.959
Aromatic	(F+H + W+Y)	42	10.825
Non-polar	(A+C + F+G + I+L + M+P + V+W + Y)	223	57.474
Polar	(D+E + H+K + N+Q + R+S + T+Z)	165	42.526
Charged	(B+D + E+H + K+R + Z)	99	25.515
Basic	(H+K + R)	46	11.856
Acidic	(B+D + E+Z)	53	13.660

In the prediction of secondary structure of protein 3ZH5, the PDBsum results are 1 sheet, 5 beta hairpins, 4 beta bulges, 6 strands, 2 helices, 11 beta turns, 1 gamma turn, and 1 disulfide bond.

The hydropathy plot shows an amino acid sequence's hydrophobic and hydrophilic propensities. Using a hydropathy scale, each amino acid has been given a hydropathy index based on its relative hydrophobicity (positive value) or hydrophilicity (negative value). In a stable protein structure, hydrophobic residues are found on the inside whereas hydrophilic residues are found on the inside.

The frequency of each amino acid residue in the protein sequence under a certain attribute is displayed in the protein statistics. EMBOSS Pepstats was used to obtain statistical data on the amino acids under conditions such as size, charge, and pH.

The protein structure had a total of 122 amino acid residues.
The isoelectric point was found to be 9.44.
The average molecular weight was 14121.13.
The average residue weight was 115.747.

Swiss ADME analysis

Drug likeness and ADMET analysis

Based on the bioavailability score, the drug similarity analysis aids in predicting the potency of the drug candidate to be an oral drug. The structural characteristics of tiny molecules serve as the foundation for the scoring criteria. To screen out tiny molecules and determine how similar they are to drugs, the Lipinski rule of five is applied. The PAINS score, which reveals substructures that exhibit robust reactions in the studies regardless of the protein target, serves as a demonstration of the medicinal chemistry features of therapeutic compounds. The requirements for physicochemical properties are lipophilicity must be −0.7–+5.0. The TPSA value should be 20–130. Sp3 hybridization should not be <0.25 and the last requirement is that rotatable bonds should not be more than 9.

Lipinski filter requirements: H bond donors must be <5, H bond acceptors must be <10, and molecular weight must be between 150 and 500 g/mol. All of the phytochemicals in the table pass the Lipinski filter

Table 2: ADME analysis

Compound	GI absorption	BBB permeability	Pgp substrate	Silicos-IT LogSw	Silicos-IT class
Murrayacinine	High	No	No	−7.02	Poorly soluble
Murrayazolinine	High	Yes	Yes	−6.87	Poorly soluble
Osthole	High	Yes	No	−5.01	Moderately soluble
Currayanine	High	No	Yes	−7.47	Poorly soluble
Murrayazolinol	High	Yes	Yes	−6.03	Poorly soluble
Mahanimbinol	High	No	No	−7.3	Poorly soluble
Murrayacine	High	Yes	Yes	−5.77	Moderately soluble
Mukoenine A	High	Yes	No	−6.04	Poorly soluble
Mukonal	High	Yes	No	−4.34	Moderately soluble
Mahanimbine	High	No	Yes	−7.47	Poorly soluble

BBB: Blood–brain barrier

Table 3: Physicochemical properties of the ligand molecules

Molecular formula	Molecular weight	Fraction Csp3	Rotatable bonds	TPSA	Lipophilicity
C23H23NO2	345.43	0.26	4	42.09	5.72
C23H27NO2	349.47	0.48	1	45.25	4.84
C15H16O3	244.29	0.27	3	39.44	3.81
C23H25NO	331.45	0.39	1	25.02	6.17
C23H25NO2	347.45	0.48	0	34.39	4.18
C23H27NO	333.47	0.3	5	36.02	7.18
C18H15NO2	277.32	0.17	1	42.09	3.77
C18H19NO	265.35	0.22	2	36.02	5.32
C13H9NO2	211.22	0	1	53.09	3.05
C23H25NO	331.45	0.3	3	25.02	6.63

Table 4: Evaluation of Lipinski filter

Ligand	Molecular weight	MLogP	H acceptors	H donors	Molar Refractivity
Murrayacinine	345.43	3.7	2	1	108.87
Murrayazolinine	349.47	3.93	2	2	107.69
osthole	244.29	2.63	3	0	72.7
Currayanine	331.45	4.73	1	1	106.02
Murrayazolinol	347.45	3.93	2	1	105.52
Mahanimbinol	333.47	4.66	1	2	110.07
Murrayacine	277.32	2.66	2	1	85.31
Mukoenine A	265.35	3.62	1	2	86.51
Mukonal	211.22	1.49	2	2	63.22
Mahanimbine	331.45	4.66	1	1	108.45

Table 5: Aggregation analysis

Compound	Cannonical SMILES	Probability score	Aggregator class
Murrayacinine	CC(=CCCC1(C=CC2=C (O1) C(=CC3=C2NC4=CC=CC=C43) C=O) C) C	0	0.052
Murrayazolinine	CC1=CC2=C (C3=C1OC4(CCC (C3C4) C (C)(C) O) C) NC5=CC=CC=C52	0	0.167
osthole	CC(=CCC1=C (C=CC2=C1OC(=O) C=C2) OC) C	0	0.151
Currayanine	CC1=CC2=C (C3=C1OC4(CCC (C3C4) C(=C) C) C) NC5=CC=CC=C52	0	0.229
Murrayazolinol	CC1=CC2=C3C4=C1OC5(CC4C (CC5O) C (N3C6=CC=CC=C62)(C) C) C	0	0.239
Mahanimbinol	CC1=CC2=C (C(=C1O) CC=C (C) CCC=C (C) C) NC3=CC=CC=C32	0	0.23
Murrayacine	CC1(C=CC2=C (O1) C(=CC3=C2NC4=CC=CC=C43) C=O) C	0	0.141
Mukoenine A	CC1=CC2=C (C(=C1O) CC=C (C) C) NC3=CC=CC=C32	0	0.19
Mukonal	C1=CC=C2C(=C1) C3=C (N2) C=C (C(=C3) C=O) O	0	0.112
Mahanimbine	CC1=CC2=C (C3=C1OC (C=C3)(C) CCC=C (C) C) NC4=CC=CC=C42	0	0.098

Table 6: TOXICITY analysis

Compound	Cannonical smiles	Predicted LD 50 (mg/kg)	Predicted toxicity class
Murrayacinine	CC(=CCCC1(C=CC2=C (O1) C(=CC3=C2NC4=CC=CC=C43) C=O) C) C	500	4
Murrayazolinine	CC1=CC2=C (C3=C1OC4(CCC (C3C4) C (C)(C) O) C) NC5=CC=CC=C52	750	4
Osthole	CC(=CCC1=C (C=CC2=C1OC(=O) C=C2) OC) C	2905	5
Currayanine	CC1=CC2=C (C3=C1OC4(CCC (C3C4) C(=C) C) C) NC5=CC=CC=C52	750	4
Murrayazolinol	CC1=CC2=C3C4=C1OC5(CC4C (CC5O) C (N3C6=CC=CC=C62)(C) C) C	750	4
Mahanimbinol	CC1=CC2=C (C(=C1O) CC=C (C) CCC=C (C) C) NC3=CC=CC=C32	2300	5
Murrayacine	CC1(C=CC2=C (O1) C(=CC3=C2NC4=CC=CC=C43) C=O) C	522	4
Mukoenine A	CC1=CC2=C (C(=C1O) CC=C (C) C) NC3=CC=CC=C32	2300	5
Mukonal	C1=CC=C2C(=C1) C3=C (N2) C=C (C(=C3) C=O) O	800	4
Mahanimbine	CC1=CC2=C (C3=C1OC (C=C3)(C) CCC=C (C) C) NC4=CC=CC=C42	4000	5

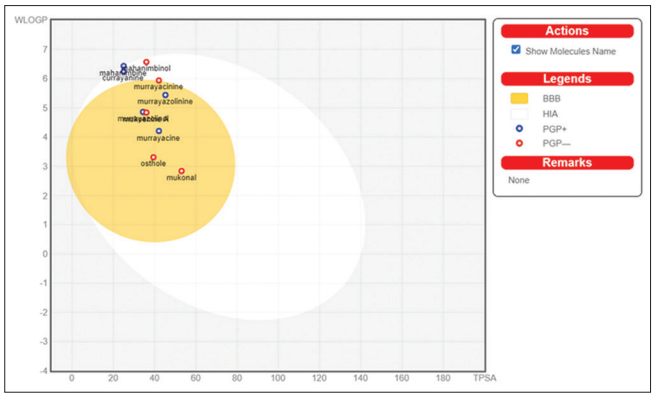

Fig. 6: Boiled-Egg assessment for the GI absorption and blood brain barrier penetration

analysis, indicating that they may have therapeutic properties because their values fall within the range that is acceptable for human usage.

Blood–brain barrier restricts the penetration of the compound into the brain.

Gastrointestinal adsorption should be high to improve the drug's efficiency.

The solubility values need to be less negative.

These values are obtained using SwissADME.

Compounds were classified as aggregators and non-aggregators using ChemAGG server.

Compounds with a probability score of zero are impossible to aggregate.

LD50 is the amount of substance administered all at once which can also lead to the death of animals.

LD50 values <50 mg/kg are known to be highly toxic.

Boiled-egg analysis

The white section (egg white) represents a greater likelihood of passive absorption through the GIT, while the yellow region (egg yolk) indicates a high potential for brain invasion. The sections of yolk and white are not mutually exclusive. The spots are also colored blue if they are projected to be effectively effluxed by PGP+and red if they are anticipated to be non-substrate of PGP. In this study, we can see that the phytocompounds Mukonal, Osthole, Murrayacine, Murrayazolinine, Murrayacinine, Murrayazolinol, and Mukoenine A falls in the yellow region which indicates these compounds have a high potential for brain invasion. Similarly, Currayanine, Mahanimbine, and Mahanimbinol fall

in the white region indicating that these compounds represent a greater likelihood of passive absorption through GIT.

Molecular docking

The binding affinity of all the selected ligands toward the 3ZH5 protein as obtained by PyRx is enlisted in Table 7.

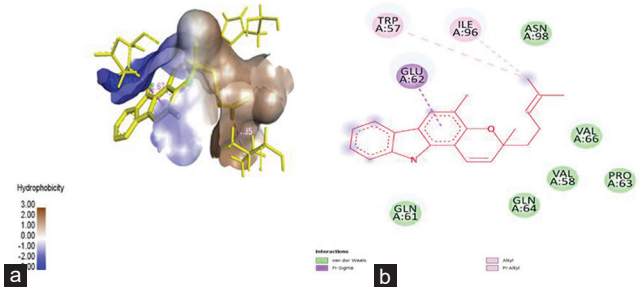

Fig. 7: visualization of molecular interactions of 3ZH5 with Mahanimbine ligand (a) 3D interaction, (b) 2D interaction

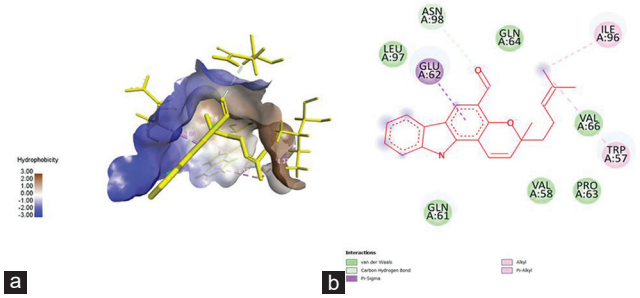

Fig. 8: Visualisation of molecular interactions of 3ZH5 with Murrayacinine ligand (a) 3D interaction, (b) 2D interaction

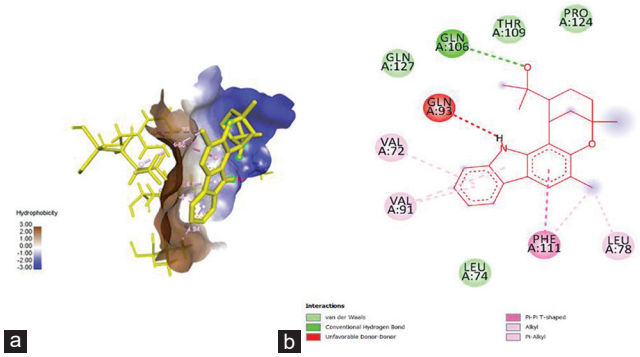

Fig. 9: Visualisation of molecular interactions of 3ZH5 with Murrayazolinine ligand

Table 7: Docking score of 3ZH5 protein E with selected ligands

Compound	Binding Affinity
Murrayazolinine	-7.4
Murrayacinine	−7.1
Osthole	−5.6
Mahanimbinol	−5.7
Mahanimbine	−7.2
Murrayazolinol	−6.9
Currayanine	−6.7
Mukonal	−5.7
Mukoenine A	−6.6
Murrayacine	−6.3

The docking conformation that yielded the highest binding energy was considered for further evaluation. In this study, the highest binding energy was seen in the phytocompounds above −7, that is, the compounds highlighted in green (Murrayacinine, Mahanimbine, and Murrayazolinine) fall in that category. Hence, these three are chosen for further analysis.

visualization

The bond types observed in this 2D interaction are Van der Waals, Pi-sigma, Alkyl, and Pi-alkyl interactions.

The bond types observed in this 2D interaction are van der Waals, Carbon Hydrogen Bond, Pi-sigma, Alkyl, and Pi-alkyl interactions.

The bond types observed in this 2D interaction are Van der Waals, Conventional Hydrogen Bond, Unfavorable Donor-Donor, Pi-Pi T-shaped, Alkyl, and Pi-alkyl.

DISCUSSION

Koch observed tiny Gram-negative rods in conjunctivitis patients' pus in 1883, marking the 1st time *H. influenzae* was recognized as a bacterium capable of causing human disease. *H. influenzae* is a Gram-negative coccobacillus. Many of the bacteria that cause serious illnesses in children have polysaccharide capsules. The bacterium may benefit from the capsule's capacity for survival by being protected during transmission and colonization as well as being resistant to complement-mediated death and phagocytosis [21]. *H. influenzae* causes many types of diseases and infections such as Otitis media [22], Bronchitis [23], Cellulitis [24], pneumonia [25], and bloodstream infection [26]. The protein 3ZH5 used in this study is a multifunctional adhesion that is involved in direct interactions with lung epithelial cells hence the diseases which affect the lungs are Bronchitis and Pneumonia.

The development of novel pharmaceuticals can be done using easily available medicinal plants, which are also a more affordable source with fewer side effects. Since ancient civilization, plant materials have been used as a significant ingredient in the synthesis of medications in various forms, such as decoctions, making plant-based traditional medicine the dominant type of healthcare in many Asian countries. The most widely used plant in Asia, curry leaves have significant medicinal and nutritional benefits. *M. koenigii* is used to treat diabetes, chronic fever, dysentery, and diarrhea with various components of the plant [27-30]. In this research, ten phytocompounds from *M. koenigii* are selected and subjected to pharmacological analysis. The ligands with the strongest binding properties are then selected. Here, the phytocompounds Murrayazolinine, Murrayacinine, and Mahanimbine have the highest binding characteristics, all of which are above -7, with Murrayazolinine having the highest binding affinity of the three, measuring at −7.4 as a result, these are sent for docking.

They serve as ligands and attach to the *H. influenzae* PE, which makes it difficult for the protein to adhere to surfaces and prevents infection. According to previous literature, Mahanimbine is a carbazole alkaloid that has been reported to be present in the plant's bark, stem, and leaves. It demonstrates a variety of qualities, including anti-tumor, anti-convulsant, and antioxidant [31]. Similarly, the novel carbazole alkaloids murrayazolinine and murrayacinine would be effective against *H. influenzae* by binding to its protein which has an indispensable role in the pathogenesis of bacterial infection [32]. Hence, these phytocompounds can be used for drug development against *H. influenzae*.

CONCLUSION

Most often affecting children, *H. influenzae* has become more prevalent during the last 20 years. To eradicate this disease, numerous vaccinations are being developed. The medicinal herbs that can be employed for the creation of drugs against *H. influenzae* are just as significant as the vaccines. *M. koenigii* is one such plant with several therapeutic qualities. In this way, with the aid of numerous studies,

better *H. influenzae* prevention and treatment can be accomplished. A significant change will occur in medicine due to the rising usage of medicinal herbs in drug development.

ACKNOWLEDGMENT

I hereby acknowledge Ms. Susha D for her guidance and BioNome for providing computational facilities and support in the scientific research services.

REFERENCES

1. Agrawal A, Murphy TF. *Haemophilus influenzae* infections in the *H. influenzae* Type b conjugate vaccine era. J Clin Microbiol 2011;49:3728-32.
2. Singh B, Al-Jubair T, Mörgelin M, Thunnissen MM, Riesbeck K. The unique structure of *Haemophilus influenzae* protein E reveals multiple binding sites for host factors. Infect Immun 2013;81:801-4.
3. Handral HK, Pandith A, Shruthi SD. A review on *Murraya koenigii*: Multipotential medicinal plant. Asian J Pharm Clin Res 2012;5:5-14.
4. Saini SC, Reddy GB. A review on curry leaves (*Murraya koenigii*): Versatile multi-potential medicinal plant. Am J Phytomed Clin Ther 2015;3:363-8.
5. Berman HM, Westbrook J, Feng Z, Gilliland G, Bhat TN, Weissig H, *et al*. The protein data bank. Nucleic Acids Res 2000;28:235-42.
6. Rose PW, Prlić A, Altunkaya A, Bi C, Bradley AR, Christie CH, *et al*. The RCSB protein data bank: Integrative view of protein, gene and 3D structural information. Nucleic Acids Res 2017;45:D271–81.
7. Burley SK, Berman HM, Kleywegt GJ, Markley JL, Nakamura H, Velankar S. Protein data bank. Nature New Biol 1971;233:223.
8. Laskowski RA, Jabłońska J, Pravda L, Vařeková RS, Thornton JM. PDBsum: Structural summaries of PDB entries. Protein Sci 2018;27:129-34.
9. Chojnacki S, Cowley A, Lee J, Foix A, Lopez R. Programmatic access to bioinformatics tools from EMBL-EBI update: 2017. Nucleic Acids Res 2017;45:W550-3.
10. Yadav RN, Agarwala M. Phytochemical analysis of some medicinal plants. J Phytol 2011;3:10-14
11. Abeysinghe DT, Kumara K, Kaushalya K, Chandrika UG, Alwis D. Phytochemical screening, total polyphenol, flavonoid content, *in vitro* antioxidant and antibacterial activities of Sri Lankan varieties of *Murraya koenigii* and *Micromelum minutum* leaves. Heliyon 2021;7:e07449.
12. Daina A, Michielin O, Zoete V. SwissADME: A free web tool to evaluate pharmacokinetics, drug-likeness and medicinal chemistry friendliness of small molecules. Sci Rep 2017;7:42717.
13. Walters WP. Going further than Lipinski's rule in drug design. Expert Opin Drug Discov 2012;7:99-107.
14. Cui Y, Desevaux C, Truebenbach I, Sieger P, Klinder K, Long A, *et al*. A Bidirectional permeability assay for beyond rule of 5 compounds. Pharmaceutics 2021;13:1146.
15. Yang ZY, Yang ZJ, Dong J, Wang LL, Zhang LX, Ding JJ, *et al*. Structural analysis and identification of colloidal aggregators in drug discovery. J Chem Inf Model 2019;59:3714-26.
16. Kemmish H, Fasnacht M, Yan L. Fully automated antibody structure prediction using BIOVIA tools: Validation study. PLoS One 2017;12:e0177923.
17. Yoshikawa N, Hutchison GR. Fast, efficient fragment-based coordinate generation for Open Babel. J Cheminform 2019;11:49.
18. Dallakyan S, Olson AJ. Small-molecule library screening by docking with PyRx. In Chemical Biology. New York: Humana Press; 2015. p. 243-50.
19. Gansukh E, Nile A, Kim DH, Oh JW, Nile SH. New insights into antiviral and cytotoxic potential of quercetin and its derivatives-a biochemical perspective. Food Chem 2021;334:127508.
20. Chandran A, Watt JP, Santosham M. Prevention of *Haemophilus influenzae* Type b disease: Past success and future challenges. Expert Rev Vaccines 2005;4:819-27.
21. Leibovitz E, Jacobs MR, Dagan R. *Haemophilus influenzae*: A significant pathogen in acute otitis media. Pediatr Infect Dis J 2004;23:1142-52.
22. Murphy TF. *Haemophilus influenzae* in chronic bronchitis. Semin Respir Infect 2000;15:41-51.
23. Veraldi S, Benzecry V. *Haemophilus influenzae* periorbital cellulitis in a 95-year-old patient. J Gerontol Geriatr 2021;69:84-6.
24. Barnes DJ, Naraqi S, Igo JD. *Haemophilus influenzae* pneumonia in Melanesian adults: Report of 15 cases. Thorax 1987;42:889-91.
25. Tam PY., Musicha P, Kawaza K, Cornick J, Denis B, Freyne B, *et al*. Emerging resistance to empiric antimicrobial regimens for pediatric bloodstream infections in Malawi (1998-2017). Clin Infect Dis 2019;69:61-8.
26. Mohanraj K, Karthikeyan BS, Vivek-Ananth RP, Chand RP, Aparna SR, Mangalapandi P, *et al*. IMPPAT: A curated database of Indian medicinal plants, phytochemistry and therapeutics. Sci Rep 2018;8:4329.
27. Abeysinghe DT, Alwis D, Kumara K, Chandrika UG. Nutritive importance and therapeutics uses of three different varieties (*Murraya koenigii*, *Micromelum minutum*, and *Clausena indica*) of curry leaves: An updated review. Evid Based Complement Alternat Med 2021;2021:5523252.
28. Gahlawat DK, Jakhar S, Dahiya P. *Murraya koenigii* (L.) Spreng: An ethnobotanical, phytochemical and pharmacological review. J Pharmacogn Phytochem 2014;3:109-19.
29. Atanasov AG, Waltenberger B, Pferschy-Wenzig EM, Linder T, Wawrosch C, Uhrin P, *et al*. Discovery and resupply of pharmacologically active plant-derived natural products: A review. Biotechnol Adv 2015;33:1582-614.
30. Yuan H, Ma Q, Ye L, Piao G. The traditional medicine and modern medicine from natural products. Molecules 2016;21:559.
31. Dahiya J, Singh J, Kumar A, Sharma A. Isolation, characterization and quantification of an anxiolytic constituent-mahanimbine, from *Murraya koenigii* Linn. Spreng Leaves. J Ethnopharmacol 2016;193:706-11.
32. Sim KM, Teh HM. A new carbazole alkaloid from the leaves of Malayan *Murraya koenigii*. J Asian Nat Products Res 2011;13:972-5.